Structural Information from Solid-State NMR

Beat H. Meier*
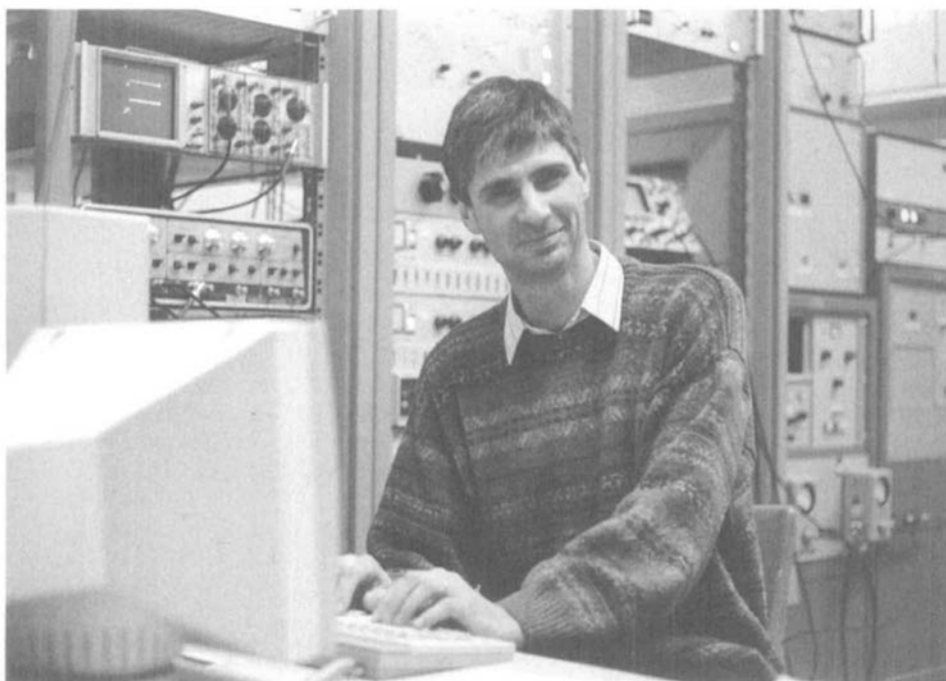
B.H. Meier. 8.9.1954: Born in Solothurn (Switzerland). 1961–1973 Primary School and Gymnasium in Gerlafingen and Solothurn. 1973–1974 Studies in Biology at the Philosophische Fakultät II, University of Zürich. 1974–1978 Studies at the Department of Chemistry, ETH-Zürich.
1978 Dipl. Chem. ETH. Diploma thesis under the direction of Prof. *R.R. Ernst*: 'Two dimensional NMR spectroscopy in systems with chemical exchange and cross relaxation'. 1979–1984: Graduate studies at the Laboratorium für Physikalische Chemie, ETH-Zürich under the direction of Prof. *R.R. Ernst* and Prof. *A. Furrer*. Title of the Ph.D. thesis: 'Dynamic and Structure of Intramolecular Hydrogen Bonds in Dimeric Carboxylic Acids: A Solid State NMR and Neutron Diffraction Study'. 1984: Dr. sc. nat. ETH-Zürich. 1984 –1986 'Director founded Postdoctoral Fellow' at Los Alamos National Laboratory, USA, in the group of Dr. *W.L. Earl.* Methodical developments in solid-state NMR spectroscopy, studies of dynamical processes in the solid. 1986–: Staff member, Laboratorium fur Physikalische Chemie, ETH-Zürich, research group of Prof. *R.R. Ernst*. Solid-state NMR, computer-simulation of spin dynamics. 1992: *Ruzicka*-Prize. 1993: Habilitation at the ETH-Zürich, Department of Chemistry. Title of the Habilitation thesis 'Polarization Transfer and Spin Diffusion in Solid-State NMR'.

Abstract. The application of selective averaging techniques combined with multidimensional spectroscopy to solid-state NMR structure determination is discussed. Examples include spin-diffusion and spy-diffusion experiments.

1. Introduction

Nuclear Magnetic Resonance (NMR) of solid materials can reveal detailed information about molecular and crystal structure and about dynamical processes. In the following we will examine some possibilities of characterizing structures with typical length scales in the range from atomic distances up to a few micrometers. Larger length scales can be investigated using NMR imaging methods (not discussed here, see *e.g.* [1]).

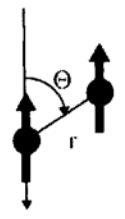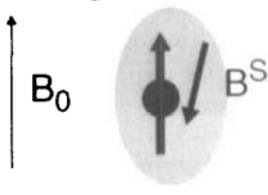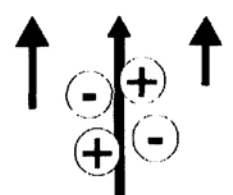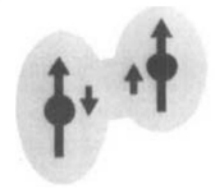The magnitude of NMR interactions falls off rapidly over a few atomic distances, and the structure is reconstructed from interactions between neighboring atoms. Long-range order is of no consequence for the experiments. NMR is, therefore, a local method for structure determination and grounds heavily on the spectral resolution of signals that origin from isotopically, chemically, or crystallographically distinct sites in the solid material. Diffraction methods, in contrast, are based on the periodic arrangement of unit cells. The more long-range order (good crystals) the better the structure can be determined.

The good success of NMR structure-determination methods in biological macromolecules in the liquid phase [2][3] clearly indicates the power of local methods for the determination of atomic resolution structures even of complicated systems. The very high spectral resolution typically encountered in liquid state spectra (with a typical ratio of linewidth to resonance frequency of 10^{-10}) is a consequence of the partial dynamic averaging of NMR interactions by the fast (on the NMR time scale) overall tumbling of the molecules in a liquid. In the solid-state, however, a straightforward (one-pulse or continuous wave) NMR experiment leads usually to a single, broad, and featureless resonance line. Starting in the late fifties [4][5], a number of schemes that selectively remove interactions and lead to high-resolution solid-state spectra have been developed [6–11]. These methods, combined with the principles of multidimensional spectroscopy [2][12–15], can be used to construct experiments that elucidate structural and dynamical properties of solid materials. A number of ingenious experiments have already been developed but much work is left to render NMR in the solid state as useful to the chemical community as liquid-state NMR already is.

The application of non-diffraction methods to structure evaluation is most useful, if the standard X-ray and neutron-diffraction techniques fail to fully determine the structure. Diffraction methods are extremely well suited to the investigation of single crystals where, in many cases, the full three-dimensional structure is obtained from a single diffraction experiment. For powdered crystalline samples, where diffraction data are averaged over the crystallite orientations, a full three-dimensional structure is only obtained in reasonably simple samples. For disordered samples (*e.g.* glasses, amorphous polymers, polymer blends, ceramics), the real

Correspondence: PD Dr. B.H. Meier
Laboratorium für Physikalische Chemie
ETH-Zentrum
CH–8092 Zürich

Table 1. *The Information Contents of Some NMR Interactions*

Interaction		Information contents	*Euler* angles	Realation to structure
		Principal values		
Dipolar		Internuclear distances	1	strict
Chemical Shielding		'Chemical environment', Coordination, Distinction of different 'sites'	3	approximate (empirical rules)
Quadrupolar		Symmetry properties of enfironment (electric field gradient) Distinction of different 'sites'	3	approximate (empirical rules)
J Coupling		Connectivity through chemical bonds (*via* electrons). Dihedral angles.	0(3)	strict (angles approximate)

space information content of the diffraction data is usually limited to the radial distribution function (RDF) [16–18]. The RDF is a one-dimensional function that describes the pair correlation of the atomic positions or the centers of the electron clouds [19]. From the pair correlation functions, it is, in general, not possible to reconstruct the three-dimensional atomic arrangement.

NMR Spectroscopy provides new information not available in diffraction experiments, because it can distinguish between different 'sites' on grounds of chemical environment, coordination, conformation, local symmetry, and orientation with respect to the external magnetic field direction. The magnetic dipole-dipole interaction and the *J*-coupling interaction allow to establish through-space and through-bond spatial relationships between these resolved sites. This information alone can, in favorable cases, be used to reconstruct the full 3D structure of the object under investigation. In disordered solids, a complete structure determination is not feasible, but valuable information, often

complementary to the one obtained by diffraction, can be provided.

Similar techniques can also be employed to obtain information about slow motional processes in solids. An overview over these techniques is found in [20].

2. Information Contents and Symmetry of NMR Interactions in Solids

While the *Zeeman* interaction with the *external* magnetic field B_0 provides only atom-type and isotope-type resolution, detailed information about the structure and dynamics of the sample is reflected in the weaker internal interactions [7][8], namely the chemical shielding σ, the *J* coupling, and the magnetic dipole-dipole interaction, and for nuclei with a spin-quantum number larger than $^1/_2$ the nuclear electric quadrupole interaction. All of these interactions are, in the solid state, anisotropic and depend on the orientation of the molecule-fixed coordinate system with respect to the magnetic field. As a simple illustration, we consider the chem-

ical shielding (CS) tensor. The spin of a given nucleus k in a sample does not experience exactly the externally applied magnetic field $\vec{B}_0$ but a field $\vec{B} = \vec{B}_0 + \vec{B}_k^S$ slightly modified in magnitude and direction due to the shielding of the external field by the neighboring electron density (see also *Table 1*). The additional field $\vec{B}_k^S$ is related to the applied field $\vec{B}_0$ through the chemical shielding tensor $\sigma^{(k)}$: $\vec{B}_k^S = \sigma^{(k)} \vec{B}_0$. In matrix notation, we find (for the static field along the z axis):

$$\begin{bmatrix} B_{kx}^S \\ B_{ky}^S \\ B_{kz}^S \end{bmatrix} = \begin{bmatrix} \tilde{\sigma}_{xx}^{(k)} & \tilde{\sigma}_{xy}^{(k)} & \tilde{\sigma}_{xz}^{(k)} \\ \tilde{\sigma}_{yx}^{(k)} & \tilde{\sigma}_{yy}^{(k)} & \tilde{\sigma}_{yz}^{(k)} \\ \tilde{\sigma}_{zx}^{(k)} & \tilde{\sigma}_{zy}^{(k)} & \tilde{\sigma}_{zz}^{(k)} \end{bmatrix} \begin{bmatrix} 0 \\ 0 \\ B_0 \end{bmatrix} \quad (1)$$

The NMR spectrum is only sensitive to the symmetrical part of the chemical shielding tensor [8] which can be characterized by six parameters (*e.g.* $\tilde{\sigma}_{xx}^{(k)}$, $\tilde{\sigma}_{yy}^{(k)}$, $\tilde{\sigma}_{xx}^{(k)}$, $\tilde{\sigma}_{xy}^{(k)}$, $\tilde{\sigma}_{xz}^{(k)}$, and $\tilde{\sigma}_{yz}^{(k)}$). $\sigma^{(k)}$ can be diagonalized by a rotation matrix R:

$$R\left(\alpha^{(k)}\beta^{(k)}\gamma^{(k)}\right)\tilde{\sigma}R^{-1}\left(\alpha^{(k)}\beta^{(k)}\gamma^{(k)}\right) = \begin{bmatrix} \sigma_{xx}^{(k)} & 0 & 0 \\ 0 & \sigma_{yy}^{(k)} & 0 \\ 0 & 0 & \sigma_{zz}^{(k)} \end{bmatrix} \quad (2)$$

where $(\alpha, \beta, \gamma,)$ denote *Euler* angles. It is often convenient to describe the CS tensor by the isotropic average $\bar{\sigma}^{(k)}$, the anisotropy $\delta^{(k)}$ and the asymmetry $\eta^{(k)}$:

$$\bar{\sigma}^{(k)} = (\sigma_{xx}^{(k)} + \sigma_{yy}^{(k)} + \sigma_{zz}^{(k)})/3$$

$$\delta^{(k)} = \sigma_{zz}^{(k)} - \bar{\sigma}^{(k)} \quad (3)$$

$$\eta^{(k)} = \left(\sigma_{yy}^{(k)} - \sigma_{xx}^{(k)}\right)/\delta^{(k)}$$

and by the three *Euler* angle $\alpha^{(k)}, \beta^{(k)}, \gamma^{(k)}$ that relate the principal axis system (PAS) of the tensor to the laboratory coordinate system. The CS tensor can be decomposed into components according to the behavior under rotations of the coordinate system (the rank k). The rank 0 component that transforms like a scalar (is invariant under any rotation R) is called the isotropic chemical shielding, the rank 2 contributions (that transform like a vector) are irrelevant as they correspond to the asymmetrical part of the CS tensor, and the rank 2 contributions are often denoted as the chemical shielding anisotropy (CSA) ten-

sor, as they express the spatial anisotropy and asymmetry of the CS tensor. The components A_{lm} of the rank l tensor A_l in its principal axis system are easily obtained from $\bar{\sigma}^{(k)}$, $\delta^{(k)}$, and $\eta^{(k)}$ by the relations $A_{00} = -\sqrt{3}\,\tilde{\sigma}^{(k)}$, $A_{20} = \sqrt{3/2}\delta^{(k)}$, and $A_{2\pm2} = \delta^{(k)}\eta^{(k)}/2$. No components of rank larger than two are found for the basic NMR interactions. If, however, a quadrupole interaction that is not very much smaller than the *Zeeman* interaction is present, forth (and higher) rank contributions are introduced. The NMR spectra depend usually only on the A_{l0} tensor components in the laboratory frame of reference. For second rank interactions,
$A_{20} = \sqrt{3/8}\delta^{(k)}[(3\cos^2\beta^{(k)}-1) + \eta^{(k)}\sin^2\beta^{(k)}\cos 2\alpha^{(k)}]$ is obtained. The angles $-\alpha$ and $-\beta$ correspond to the polar angles of the magnetic field vector in the

PAS of the interaction considered and the orientational dependence of the interaction can be graphically represented as shown in *Fig. 1*, where the size of the interaction for a given orientation of the magnetic field vector relative to the PAS is the length of the vector from the origin of the PAS to the indicated surface. For axially symmetric tensors ($\eta = 0$) each resonance frequency in the powder pattern found in the NMR spectrum can be assigned unambiguously to a single orientation of the unique principal axis of the tensor and the direction of the static magnetic field (characterized by the *Euler* angle β). This assignment is illustrated in *Fig. 2* For $\eta \neq 0$, the assignment is, in general, not unique.

Table 1 presents an overview of NMR interactions. Geometrical information is provided by the two-spin interactions, namely the dipolar interaction that yields the 'through-space' distances and the J coupling that indicates that the coupled nuclei are connected through one (or several) chemical bonds. The one-spin interactions (chemical shielding and quadrupole interactions) are primarily useful to
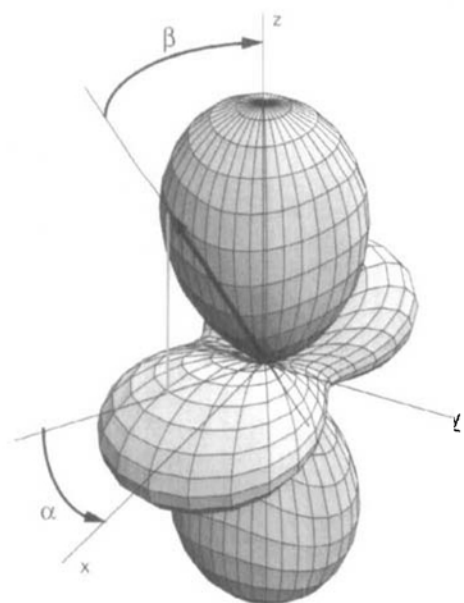

Fig. 1. *Graphical representation of the orientational dependence of a second-rank NMR interaction.* Note that the lobe along the z-axis and the lobe in the xy-plane have a different sign, leading to a vanishing isotropic average.
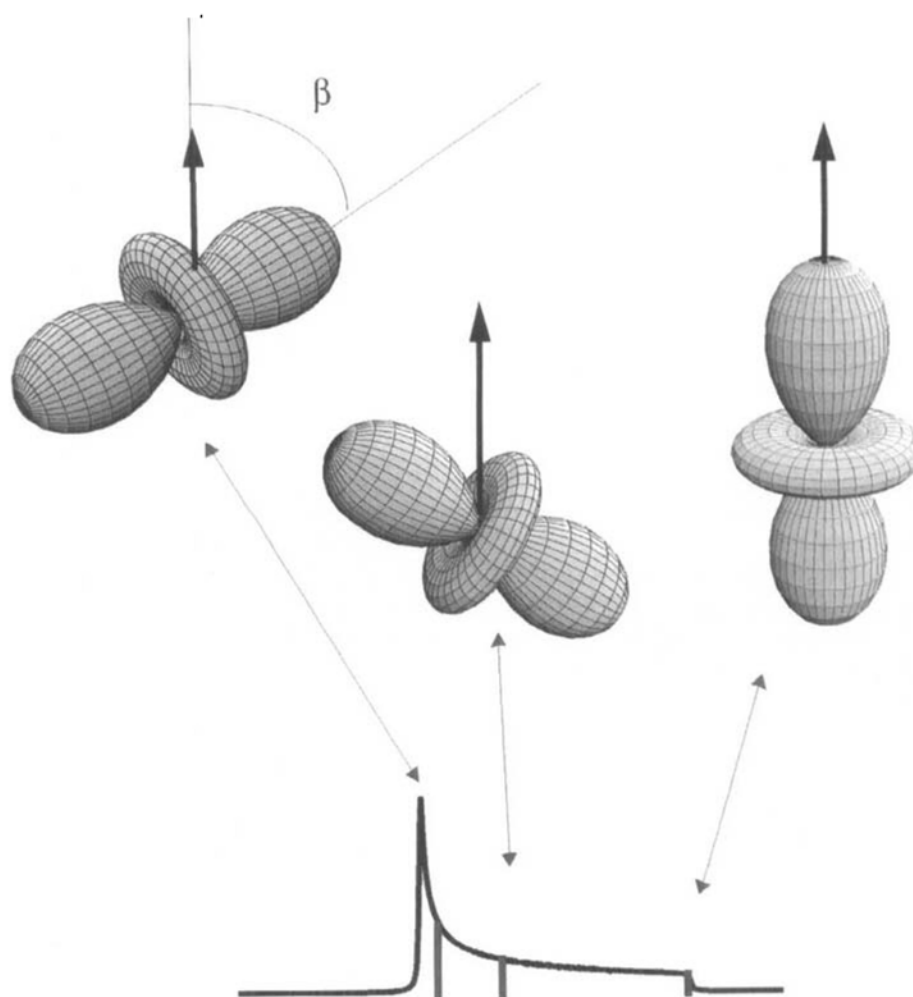

Fig. 2. *Correspondence between the* Euler *angle β and the resonance frequency for an axially symmetric CSA tensor*

provide the spectral resolution of different sites and to provide a coordinate system for correlation experiments. Through empirical rules (see *e.g.* [8][21]) the one-spin interactions can characterize the chemical identity, coordination number, and local symmetry of a site. The symmetry properties of these four interactions under rotations in real space (sample rotations) are indicated in *Table 2*. Similarly, the behavior of the interactions under rotations in spin space (application of radiofrequency pulses) can be characterized (see *Table 3*).

3. 2D Correlation Maps and Spin Diffusion

In a one-dimensional NMR experiment of a disordered or polycrystalline sample, the orientational information contained in the *Euler* angles that relate the PAS of a one-spin interaction and the laboratory coordinate system cannot be exploited, because the measured magnetization is an isotropic average over all possible orientations. In a two-dimensional experiment, it is, however, possible to determine the *relative* orientation of different sites, provided a mechanism for polarization transfer between the sites exists.

The basic scheme for such an experiment is shown in *Fig. 3*. During the evolution time t_1, the initial state of the magnetization is characterized. Each site is labelled by its resonance frequency. During the mixing time, the magnetization is transferred to neighboring sites (see below) whose resonance frequency is determined during the detection time t_2. As illustrated in *Fig. 3*, the resulting 2D frequency-domain spectrum provides a pair-correlation map of sites that can exchange their magnetization. The correlation map for a disordered sample where the PAS takes all possible orientations with respect to the external field, is sketched in *Fig. 4*. For simplicity, it describes the correlation between two sites only. The CS tensors are assumed to be axially symmetric with identical principal values. The principal axis systems, however, differ. The relative tensor orientation (the relative orientation of the two PAS) for this special case is characterized by a single *Euler* angle (β), that can be evaluated from the pair-correlation map. The correlation of two general second rank tensors allows for the determination of three *Euler* angles, the correlation of a general with an axially symmetric tensor for two *Euler* angles and the correlation of two axially symmetric tensors for one *Euler* angle.

Table 2. *Symmetry Properties of NMR Interactions under (Spatial) Sample Rotations*
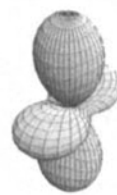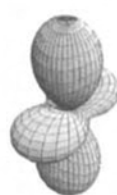

Interaction	Spatial symmetry		
	Rank 0	Rank 2	Rank 4
Dipolar		axially symmetric	
Chemical Shielding			
Quadrupolar			
J Coupling		difficult to observe	

Table 3. *Symmetry Properties of NMR Interactions under Spin Rotations*

Interaction	Symmetry under spin rotations			
	Rank 0	Rank 1	Rank 2	Rank 4
Dipolar			yes	
Chemical Shielding		yes		
Quadrupolar			yes	second order
J Coupling	yes		yes	

A mechanism for the exchange of magnetization between neighboring sites can be provided by the *J* coupling or the dipolar interaction, the latter typically being stronger by two to three orders of magnitude. In a complicated network of many coupled spins, the spatial evolution of the magnetization is approximately described by a diffusion equation.

The 2D CS-tensor correlation spectrum of a powder sample of crystalline benzoic acid, ^{13}C enriched at the carboxylic position, is reproduced in *Fig. 5*. The spectra have been recorded at long mixing times where spin diffusion has proceeded to completion and represent a pair-corre-

lation map of nuclei that belong to the same microcrystallite. Benzoic acid crystallizes in the space group $P2_1/c$ with two centrosymmetric dimers per unit cell. As a consequence of the center of symmetry, carbon sites within the same dimer are not distinguishable by NMR (see *Table 2* where the symmetry of the interaction is given). Dimers that are related by the two-fold screw axis have CS-tensors with identical principal values but different principal axis directions. From the spectra of *Fig. 5*, the three *Euler* angles between the PAS at the two sites can be extracted by a least-squares fit of the experimental lineshape [22]. The best fit is shown in *Fig. 5*.

It is illuminating to describe the relative tensor orientation as a rotation by an angle φ_P around an axis specified by the polar coordinates θ_P and ϕ_P. These three parameters are listed, as a function of temperature, in *Table 4*. It is apparent that, within experimental error, the angle φ_P equals 180° for all temperatures as expected from the crystallographic screw axis. The strong temperature dependence of ϕ_P is a consequence of the tautomeric dynamic equilibrium depicted in *Fig. 6* and can be exploited to determine the asymmetry of the double-minimum potential (*Fig. 6*) to 418±128 J/mol [23].

Fig. 3. *Basic scheme of the exchange experiment* [14]

Fig. 4. *CSA-Correlation map for the special case of two axially symmetric tensors with identical principal values but different principal axes directions*

4. Selective Averaging

In the above example, the spectral resolution has been obtained through selective isotopic enrichment. In a non-enriched sample, strong overlap between the seven chemically nonequivalent carbon sites in a dimer prevents a simple analysis of the experimental spectra.

Andrew and coworkers [4] and *Waugh* and coworkers [5] were the first to realize that the symmetry properties of the NMR interaction under rotations in real space and in spin space can be exploited to selectively average out parts of the interactions while retaining others. The discussion of the symmetry properties of the spin- and spatial tensors provides an elegant illustration of the possibilities of selective averaging [10][11]. Cyclic motions in either space are described by a subgroup of the full rotation group in three dimensions, SO(3). The averaging of terms of rank k according to the symmetry of the motion has been discussed by *Pines* and coworkers [10][11]. Some results are summarized in *Table 5*. Averaging in spin space is usually obtained by multiple pulse sequences that, most often, correspond to averaging over a number of discrete orientations in spin space. In real space, however, it is technically most favorable to perform the averaging by a continuous motion of the sample in three-dimensional space. The best known example is magic angle sample spinning where an octahedral symmetry is obtained by a continuous motion around an axis inclined by 54.74° with respect to the static magnetic field. Recently, two ingenious continuous schemes to obtain icosahedral symmetry have been developed, double angle spinning [24] and double rotation [25]. It should be pointed out that averaging in spin space and real space is usually not equivalent. The chemical shielding interaction, *e.g.*, is reduced to its isotropic value by appropriate spatial averaging, whereas the chemical shielding interaction is eliminated altogether by spin-space averaging.

5. Spin Diffusion

As already mentioned, spin diffusion provides a mechanism to correlate sites in spatial proximity. The so-called flip-flop term of the dipolar *Hamiltonian* ($I_1^+ I_2^- + I_1^- I_2^+$) exchanges the polarization (magnetization) of two spins with a rate constant W proportional to the square of the dipolar interaction (the inverse sixth power of the internuclear distance r) and to the probability that the two spins have the same resonance frequency:
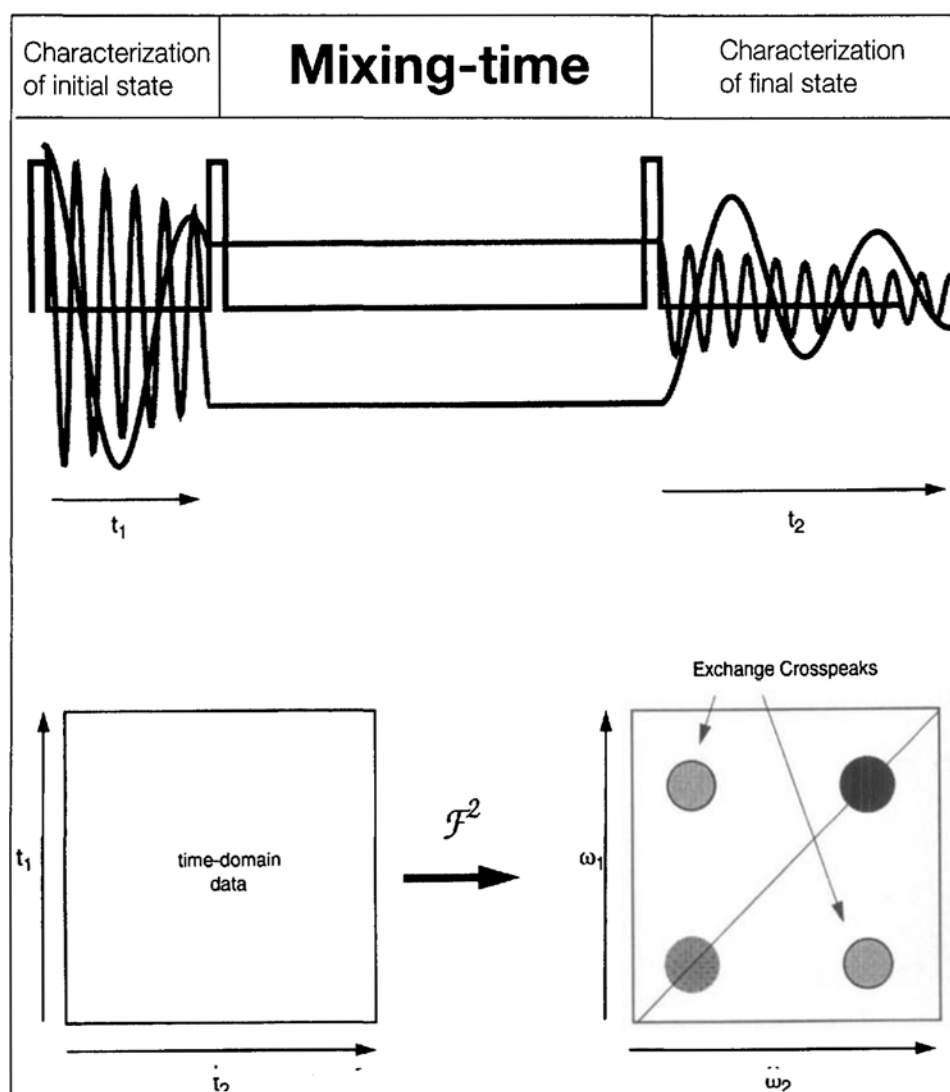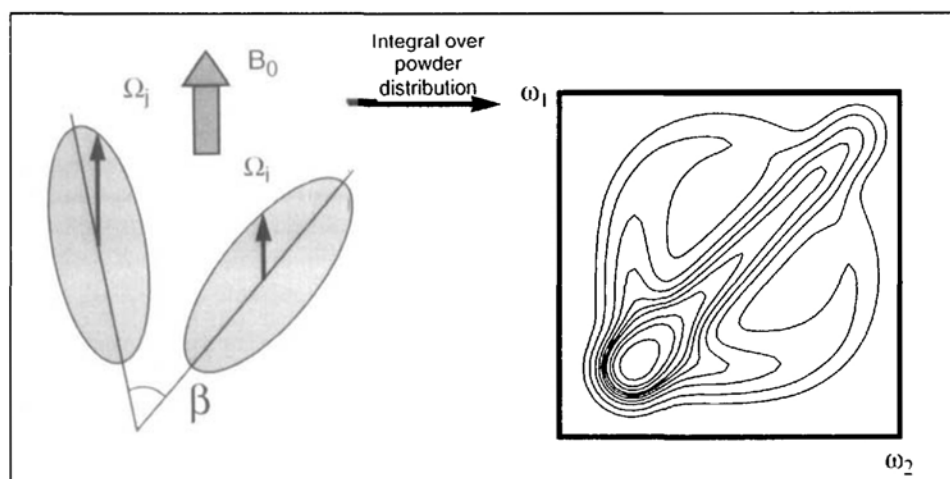
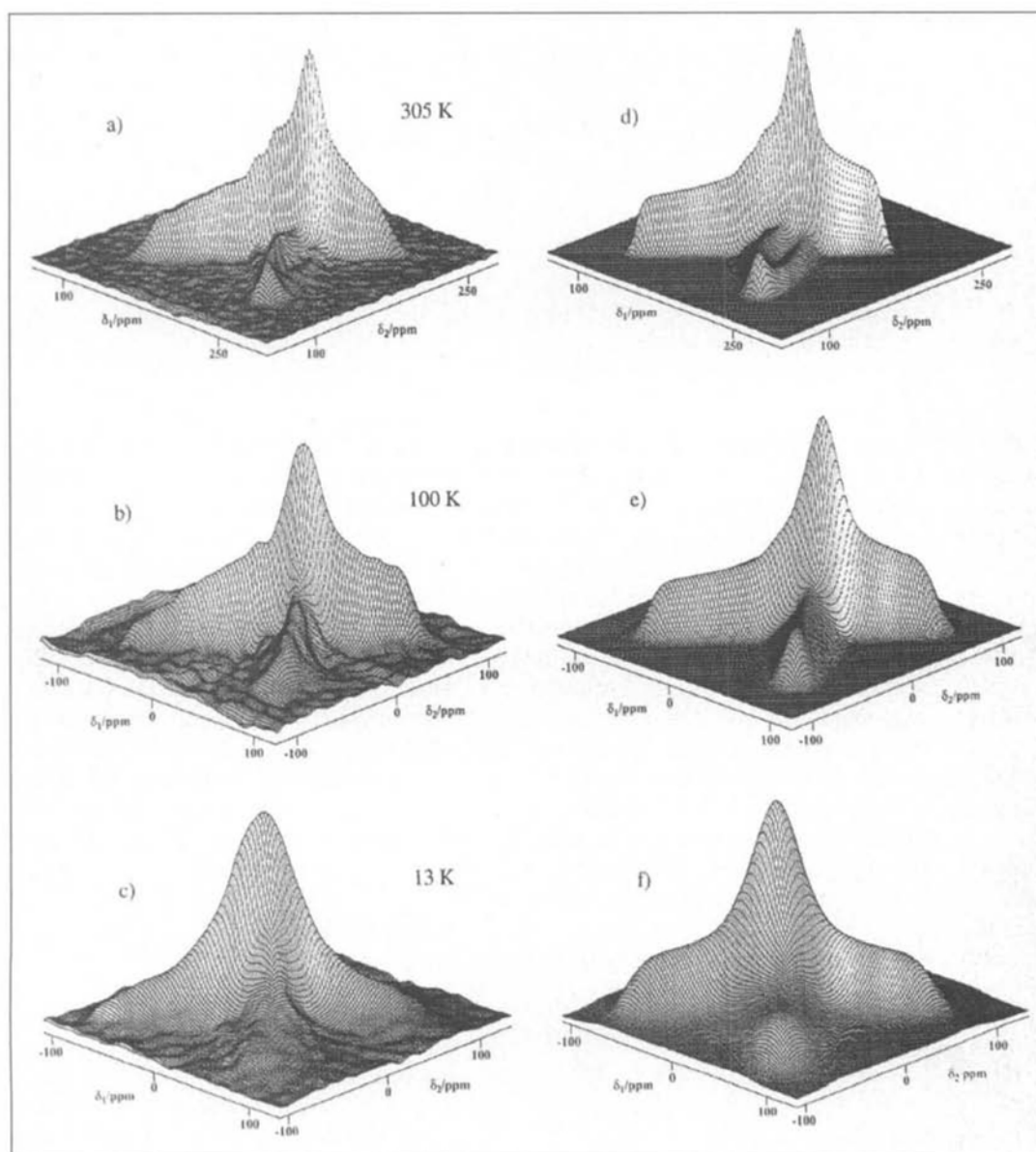Fig. 5. *Spin-diffusion spectra of benzoic acid as a function of temperature.* Experimental spectra are given to the left (*a–c*), the best theoretical fit to these spectra to the right (*d–f*) (adapted from [23]).

$$W = \frac{\mu_0^2 \hbar^2 \gamma^4}{32 \pi r^6} g(0) \qquad (4)$$

γ denotes the gyromagnetic ratio and $g(0)$ is a measure for the probability that the two spins have the same resonance frequency [26]. The second contribution is roughly equivalent to the overlap between the resonance lines of the two sites. Spin diffusion is a rather slow process. The highest diffusion constants are found for abundant spins with high gyromagnetic ratio and small chemical shielding differences (*e.g.* protons) where typical diffusion constants $D = Wr^2$ of the order of magnitude 10^{-12} cm^2/s are found [27][28]. In 1 s, the transport of magnetization extends over *ca.* a hundred inter-atomic distances. Lower isotopic abundance (larger internuclear distances), lower gyromagnetic ratios and better spectral separation

Table 4. *Angles Connecting the PAS of the Carboxyl ^{13}C CSA Tensors in the Two Magnetically Inequivalent Sites of Benzoic Acid* (from [23])

T/K	θ_ρ/deg	Φ_ρ/deg	ρ_ρ/deg
305	133.3±0.5	–15.6±1.8	180.0±2.4
100	132.2±0.6	–0.5±3.2	178.1±4.3
71	130.5±0.8	3.8±3.2	179.6±4.1
32	129.9±0.8	16.4±2.5	179.9±3.2
13	130.8±0.8	15.4±2.8	179.5±3.7

Table 5. *Averaging of Tensor Interactions of Rank k by Symmetry Operations under Relevant Subgroups of the Full Rotation Group*

Symmetry		Tensor Ranks that Survive Averaging		
Tetragonal	D$_4$	0	2	4
Tetrahedral	T	0		4
Octahedral	O	0		4
Icosahedral	I	0		
Spherical	SO(3)	0		

Table 6. *Averaging Schemes Applied in the Experiment of* Fig. 7

	Evolution	Mixing	Detection
Averaging Scheme	MAS (spatial)	Rf-Irradiation (spin-space)	MAS (spatial)
Interactions Averaged	Chemical Shielding Anisotropy Dipolar Interaction	Chemical Shielding	Chemical Shielding Anisotropy Dipolar Interaction
Remaining Interactions	Isotropic Chemical Shielding	Dipolar Interaction	Isotropic Chemical Shielding

degrade the spin-diffusion rate. Furthermore, in resolved spectra, the diffusion rate is a function of the chemical shielding difference between the involved nuclei and can be too low to be observed in well resolved spectra. To enhance the spin-diffusion rate in the case of resolved spectra and to render it independent of the spectral parameters, a number of driven spin-diffusion schemes have been developed [29–33]. These methods use an external 'heat bath' to provide the necessary energy for a flip-flop transition in a coupled spin pair.

Proton spin diffusion is particularly useful to investigate structures with relatively large mean distances between sites, *e.g.* the miscibility of polymer blends [28][34], while the observation of driven spin diffusion between rare spins (*e.g.* ^{13}C) is useful to establish the relative orientation of neighboring units in disordered systems and for systems where the resolution in the proton spectrum is not sufficient. *Fig. 7* shows an rf-driven spin-

diffusion spectrum (using a continuous wave spin lock) of a macroscopic and a molecular mixture of adamantane and hexamethylethane. To obtain the desired spectral resolution during evolution and detection and to facilitate spin diffusion during mixing, selective averaging schemes have been applied during the three periods as shown in *Table 6*. During evolution and detection, MAS is employed to obtain high-resolution spectra. During mixing when spin diffusion takes place, the spatial averaging by MAS is inhibited by an alignment of the spinning axis parallel to the direction of the static magnetic field [33]. From the presence of spin-diffusion

cross-peaks between the two components in one of the two samples and from their absence in the other it is obvious that the two components are once mixed on a molecular level and well separated in the other case.

For isolated pairs of spins, the magnetization transfer is oscillatory and the oscillation frequency can be used to determine the internuclear distance. Of particular interest in this context are MAS experiments (rotational resonance) that allow for accurate distance determinations in doubly labelled samples [30][35][36].

6. Spy Diffusion

In the preceding chapter, the 'diffusion' of magnetization between spins that remain at a fixed position (spin diffusion) has been exploited. Spin diffusion is limited to investigations that involve distances smaller than *ca.* 100 nm. As an alternative to these experiments, it is possible to introduce mobile magnetic 'spy' nuclei and to follow their spatial diffusion. Due to its high polarizability, its chemical inertness and the relatively high gyromagnetic ratio, ^{129}Xe is a particularly suitable spy nucleus. The chemical shielding of xenon depends on its chemical environment. It is, *e.g.*, easily possible to distinguish Xe dissolved in poly(methyl vinyl ether) and polystyrene. This chemical shielding difference provides the necessary resolution to monitor the diffusion of xenon atoms (carrying their magnetization) between the components of the blend obtained from the polymers mentioned above. Using the exchange scheme of *Fig. 3*, the diffusion of xenon in a laminar blend of the two polymers has been investigated [37]. The 2D exchange spectrum for different mixing times is shown in *Fig. 8*. From the buildup of the cross-peak intensity, the exchange rate constant k can be determined which, for a laminar blend, is related to the thickness a of the lamella by the relation
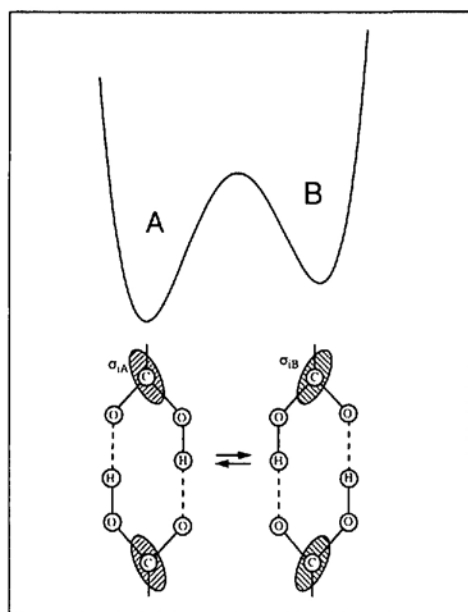
Fig. 6. *Proton exchange between the two tautomeric forms of benzoic acid.* The asymmetry of the potential is a consequence of crystal packing forces [39].
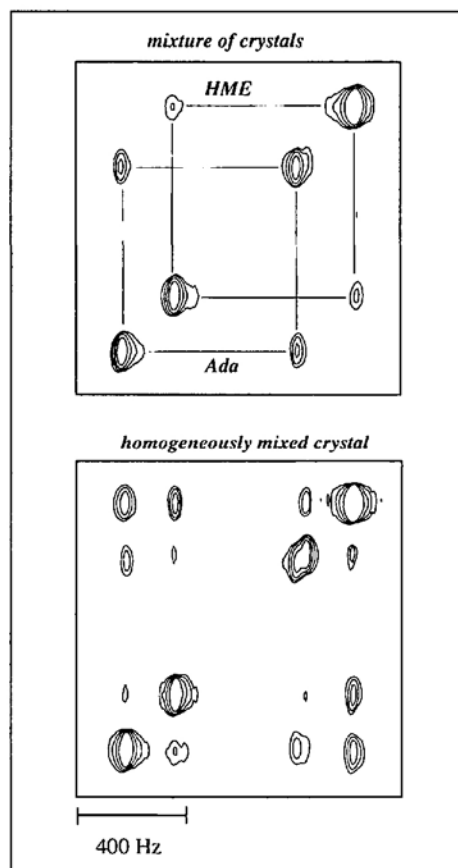
400 Hz

Fig. 7. *Spin-diffusion spectra* (^{13}C) *for a macroscopic and molecular mixture of adamantane and hexamethylethane.* Cross peaks between resonances indicate spatial proximity of the nuclei (Courtesy of *Marco Tomaselli*).

$$a = \frac{6D_{eff}}{k} \qquad (5)$$

where the effective diffusion constant can be computed from to the diffusion constants of the pure components D_a and D_b and their populations p_a and p_b by:

$$D_{eff} = \frac{2p_a D_a p_b D_b}{p_a D_a + p_b D_b} \qquad (6)$$

Similar experiments have also been performed in 'regular' polymer blends [38].

7. Summary

The combination of selective averaging techniques with multidimensional spectroscopy allows for the development of solid state NMR experiments that provide structural information in the range from atomic distances up to a few micrometers. Promising applications in particular to amorphous and vitreous samples and to partially disordered crystalline materials have already been performed or can be envisioned.
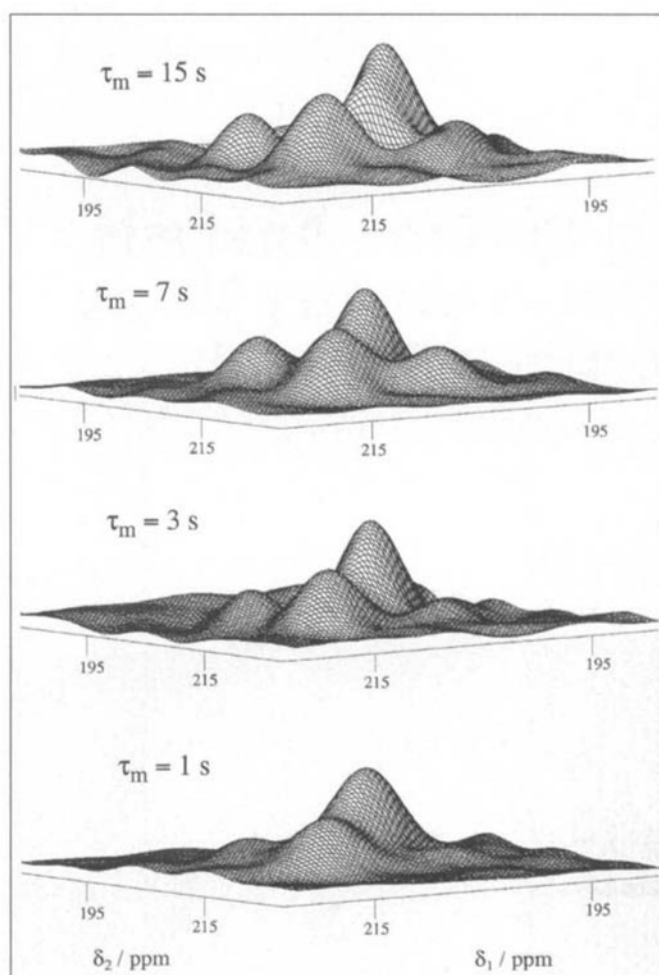
Fig. 8. *Experimental 2D exchange spectra of xenon in a laminar blend of poly(vinyl methyl ether) and polystyrene at 294 K. The mixing times employed are indicated in the figure (adapted from [37]).*

[1] 'Magnetic Resonance Microscopy', Eds. B. Blümich and W. Kuhn, VCH, Weinheim, 1992.

[2] R.R. Ernst, G. Bodenhausen, A. Wokaun, 'Principles of Nuclear Magnetic Resonance in One and Two Dimensions', Clarendon Press, Oxford, 1987.

[3] K. Wüthrich, 'NMR of Proteins and Nucleic Acids', Wiley Interscience, New York, 1986.

[4] E.R. Andrew, A. Bradbury, R.G. Eades, *Nature (London)* **1958**, *182*, 1659.

[5] J.S. Waugh, L.M. Huber, U. Häberlen, *Phys. Rev. Lett.* **1968**, *20*, 180.

[6] J.S. Waugh, *Anal. Chem.* **1993**, *65*, A725.

[7] U. Häberlen, 'High Resolution NMR in Solids: Selective Averaging', Academic Press, New York, 1968.

[8] M. Mehring, 'Principles of High Resolution NMR in Solids', 2nd edn., Spinger, Berlin, 1983.

[9] C.A. Fyfe, 'Solid State NMR for Chemists', C.F.C. Press, Guelph, Canada, 1983.

[10] A. Pines, 'NMR in Physics, Chemistry, and Biology: Illustrations of *Bloch*'s Legacy', Ed. W. Litde, Proceedings of the Bloch Symposium, Vol. 4 of *Int. J. Mod. Phys. B*, pages 1241–1267, 1992.

[11] E.W. Wooten, K.T. Mueller, A. Pines, *Acc. Chem. Res.* **1992**, *25*, 209.

[12] R.R. Ernst, *Angew. Chem.* **1992**, *104*, 817.

[13] J. Jeener, Ampere International Summer School, Basko Polje, Jugoslavia, 1971, unpublished.

[14] J. Jeener, B.H. Meier, P. Bachmann, R.R. Ernst, *J. Chem. Phys.* **1979**, *71*, 4546.

[15] B.H. Meier, R.R. Ernst, *J. Am. Chem. Soc.* **1979**, *101*, 6441.

[16] A.C. Wright, *J. Non-Cryst. Solids* **1990**, *123*, 129.

[17] H.P. Klug, L.E. Alexander, 'X-Ray Diffraction Procedures for Polycrystalline and Amorphous Materials', 2nd edn., Wiley Interscience, New York, 1974.

[18] S.R. Elliot, *J. Non-Cryst. Solids* **1990**, *123*, 149.

[19] For samples with n atom-types the pair correlation function consist of a $n(n-1)/2$ partial correlation functions that have to be obtained from an equal number of different diffraction experiments.

[20] B. Blümich, A. Hagemeyer, D. Schaefer, K. Schmidt-Rohr, H.W. Spiess, *Adv. Materials* **1990**, *2*, 72.

[21] E. Pretsch, J.T. Clerc, J. Seibl, W. Simon, 'Tabellen zur Strukturaufklärung organischer Verbindungen mit spektroskopischen Methoden', Springer, Berlin, 1981.

[22] S. Smith, T. Levante, B.H. Meier, R.R. Ernst, *J. Magn. Reson. A* **1994**, *106*, 75.

[23] P. Robyr, B.H. Meier, R.R. Ernst, *Chem. Phys. Lett.* **1991**, *187*, 471.

[24] K.T. Mueller, B.Q. Sun, G.C. Chingas, J.W. Zwanziger, T. Terao, A. Pines, *J. Magn. Reson.* **1990**, *86*, 470.

[25] A. Samoson, A. Pines, *Rev. Sci. Instr.* **1989**, *60*, 3239.

[26] D. Suter, R.R. Ernst, *Phys. Rev. B Condens. Matter* **1985**, *32*, 4905.

[27] A. Abragam, 'The Principles of Nuclear Magnetism', Clarendon Press. Oxford, 1961.

[28] J. Clauss, K. Schmitt-Rohr, H.W. Spiess, *Acta Polymer* **1993**, *44*, 1.

[29] M.G. Colombo, B.H. Meier, R.R. Ernst, *Chem. Phys. Lett.* **1988**, *146*, 189.

[30] D.P. Raleight, M.H. Levitt, R.G. Griffin, *Chem. Phys. Lett.* **1988**, *146*, 71.

[31] P. Robyr, B.H. Meier, R.R. Ernst, *Chem. Phys. Lett.* **1989**, *162*, 417.

[32] A.E. Bennett, J.H. Ok, R.G. Griffin, S. Vega, *J. Chem. Phys.* **1992**, *96*, 8624.

[33] B. H. Meier, *Adv. Magnet. and Optical Reson.* **1993**, *18*, in press.

[34] P. Caravatti, P. Neuenschwander, R.R. Ernst, *Macromolecules* **1985**, *18*, 119.

[35] A. E. McDermott, F. Creuzet, R.G. Griffin, L.E. Zawadzke, Q.-Z. Ye, C.T. Walsh, *Biochemistry* **1990**, *29*, 5767 .

[36] F. Creuzet, A.E. McDermott, R. Gebhard, K. van-der Hoef, M.B. Spijker-Assink, J. Herzfeld, J. Lugtenburg, M.H. Levitt, R.G. Griffin, *Science* **1991**, *251*, 783.

[37] M. Tomaselli, B.H. Meier, P. Robyr, U.W. Suter, R.R. Ernst, *Chem. Phys. Lett.* **1993**, *205*, 145.

[38] M. Tomaselli, B.H. Meier, P. Robyr, U.W. Suter, R.R. Ernst, to be published.

[39] B.H. Meier, F. Graf, R.R. Ernst, *J. Chem. Phys.* **1982**, *76*, 767.